Supplemental information to the manuscript:

Differential subcellular recruitment of monoacylglycerol lipase generates spatial specificity of 2-arachidonoyl glycerol signaling during axonal pathfinding

(*Abbreviated title*: *Metabolic control of 2-AG signaling in axons*)

Erik Keimpema[1,*], Klaudia Barabas[1,*], Yury M. Morozov[2], Giuseppe Tortoriello[1], Masaaki Torii[2], Gary Cameron[3], Yuchio Yanagawa[4,5], Masahiko Watanabe[6], Ken Mackie[7] and Tibor Harkany[1,8,$]

[1]European Neuroscience Institute at Aberdeen & [3]Division of Applied Medicine, Aberdeen AB25 2ZD, United Kingdom; [2]Department of Neurobiology, Kavli Institute for Neuroscience, Yale University School of Medicine, New Haven, CT06510, USA; [4]Department of Genetic and Behavioral Neuroscience, Gunma University Graduate School of Medicine, 3-39-22 Showa-machi, Maebashi 371-8511, Japan; [5]Japan Science and Technology Agency, Sanbancho, Chiyoda-ku, Tokyo 102-0075, Japan; [6]Department of Anatomy, Hokkaido University School of Medicine, Sapporo 060-8638, Japan; [7]Gill Center for Neuroscience and Department of Psychological & Brain Sciences, Indiana University, 702 N Walnut Grove Avenue, Bloomington, IN 47405, USA and [8]Division of Molecular Neurobiology, Department of Medical Biochemistry & Biophysics, Karolinska Institute, S-17177 Stockholm, Sweden

* These authors contributed equally to the present work.

This file contains:

Author contributions

T.H. and Y.M.M. designed experiments. E.K. and K.B. performed multiple immunofluorescence histochemistry, knock-out analysis and western blotting. E.K. and G.T. contributed with *in vitro* cell biology, generated $CB_1R^{-/-}$ embryos, and performed real-time PCR. Y.M.M. and M.T. performed electron microscopy and electroporation, respectively. G.C. determined 2-AG levels. M.W. and K.M. contributed immunoreagents. Y.Y. provided GAD67-GFP (Δneo) mice. E.K., K.B., K.M. and T.H. wrote the manuscript. All authors have reviewed and commented on the manuscript.

A brief overview of forebrain development: putative roles of 2-AG

Forebrain development commences when telencephalic vesicles are formed with neural stem cells (NSCs) lining their walls. By embryonic day (E) ~10 in the mouse, the telencephalic NSC pool rapidly expands in the cortical neuroepithelium and commits postmitotic neurons, primordial pyramidal cells, to populate the preplate by E11 (Molnar et al., 2006). Continuous radial migration of pyramidal cells allows the cortical plate to form such that by E14 it hosts the cell dense marginal and superficial zones and the subplate, a transient compartment for thalamocortical axons (TCAs) to temporarily reside before innervating their cortical targets (Bicknese et al., 1994). Meanwhile, pyramidal cell axons grow in the intermediate zone (De Carlos and O'Leary, 1992). The first contingent of tangentially-migrating GABAergic interneurons born in the ganglionic eminences (GEs) invades the cerebrum by E12 with subsequent layer patterning achieved through radial migration from ~E15 (Tanaka et al., 2003). Neurons populating the hippocampus are generated in a similar sequential fashion (Pleasure et al., 2000). Pyramidal cells are generated between E14-18, when CB_1R^+ GABAergic interneurons already populate this region (Morozov et al., 2009), and extend their axons in the fimbria hippocampi by ~E15.

2-AG signaling is significantly different in NSCs and postmitotic neurons: NSCs possess low CB_1R expression (Aguado et al., 2005) while their DAGLα/β activity is generally high both *in vitro* and *in vivo* (Goncalves et al., 2008; Walker et al., 2009b). Neuronal commitment up-regulates CB_1R expression (Begbie et al., 2004). Conversely, DAGL expression is suppressed in cells undergoing GABAergic lineage commitment *in vitro* (Walker et al., 2009a). The canonical view on neurodevelopmental DAGL expression (Brittis et al., 1996; Bisogno et al., 2003) suggests that DAGLβ is the primary 2-AG synthetic enzyme in embryonic brain and selectively enriched in telencephalic axonal tracts. In contrast, DAGLα is considered to be the predominant postnatal DAGL isoform (Bisogno et al., 2003; Yoshida et al., 2006) with limited data available on its developmental expression. Similarly, the developmental dynamics of CRIP1a and MGL expression are unknown.

Nomenclature of anatomical structures used in this report[1]

1n	olfactory (1st) nerve	IZ	intermediate zone
2n	optic nerve	lot	lateral olfactory tract
5Gn	trigeminal ganglion	ls	lateral septum
5man	mandibular trunk of the trigeminal nerve	lv	lateral ventricle
		MZ	marginal zone
3V	third ventricle	n	nucleus
5mx/inf	infraorbital nerve, branch of the trigeminal nerve maxillary division	ne	neuroepithelium
		och	optic chiasm
		os	optic stalk
a	axon	PB/MiTg	parabrachial/microcellular tegmental nucleus
CA1-CA3	hippocampal area CA1-3 (Ammon's horn)	ppl	preplate
		pst	postsynaptic target
CP	cortical plate	SC	colliculus superior
cpu	striatum (caudate putamen)	sdz	striatal differentiation zone
CFA	corticofugal axon	sep	septum
ctx	cerebral cortex	SP	subplate
d	dendrite	sp5	spinal trigeminal tract
dmf	dorsomedial division of fimbria	SVZ	subventricular zone
f	fimbria hippocampi	TCA	thalamocortical axon
fil	filopodium	th	thalamus
gc	growth cone	vlf	ventrolateral division of fimbria
ge	ganglionic eminence	VZ	ventricular zone
hc	hippocampus		
IC	inferior colliculus		
if	intermediate division of fimbria		

[1]We have applied the nomenclature of Jacobowitz and Abbott (Jacobowitz and Abbott, 1997) to describe neural structures in the developing mouse brain.

Legends to Supporting Figures and Table

Table S1 **List of markers used for immunofluorescence labelling.** (A,A_1) Panels of antibodies applied to study the molecular composition and cell-type-specificity of 2-AG signaling in developing mouse brain. Staining methods (Harkany et al., 2003; Riedel et al., 2002) and antibody specificities were described in detail elsewhere unless stated otherwise. Table (A) and (A_1) list antibodies against molecular constituents of 2-AG signaling networks (Uchigashima et al., 2007; Mulder et al., 2008; Katona et al., 2006; Yoshida et al., 2006; Berghuis et al., 2007; Straiker et al., 2009) and neuronal identity markers (Keays et al., 2007; Sabo and McAllister, 2003; Barbin et al., 2004; Berghuis et al., 2007), respectively. Synaptic S.: Synaptic Systems GmbH.

Fig. S1 **Quality control of rabbit anti-CRIP1a antibody**. (A) The specificity of our antibody raised against the full-length CRIP1a protein has been validated by Western analysis (calculated molecular size: 18 kDa; www.ensembl.org) and (B-B_2) by eliminating CRIP1a

immunoreactivity in HEK293 cells transiently transfected with hemagglutinin (HA)-tagged CRIP1a when the polyclonal antibody has been preadsorbed with its cognate protein (FP).

Fig. S2 **Histochemical validation of antibodies.** (A-D') Histochemical controls confirming the specificity of affinity-purified antibodies used in the present report include 1) testing in knock-out mice (CB_1R (A')) or 2) comparing antibodies raised against distinct epitopes of a protein (B,B'; C,C'). Specificity of our detection systems has been established by the lack of immunoreactivity in the absence of any of the primary antibodies applied (D,D'). Solid and open arrowheads point to the presence and lack of specific immunoreactivity, respectively. (E) Western analysis of a novel antibody raised in guinea pig against DAGLα demonstrates that this antibody recognizes its protein target in heterologous expression systems using V5-tagged DAGLα (epitope tags were visualized by applying mouse anti-V5 antibody [Sigma]). Preadsorbtion experiments were performed by using corresponding fusion proteins (FP) at a concentration of 5 µg/ml. Abbreviations: Supplemental information text. *Scale bars* = 50 µm.

Fig. S3 **Cellular MGL distribution as revealed by a novel antibody raised against MGL's N-terminal 1-35 amino acid fragment**. The characteristic axonal staining pattern revealed by the affinity-purified polyclonal antibody raised against MGL's AA171-206 epitope (Figs. 6-9) has been confirmed by showing that an alternative antibody raised against MGL's N-terminal extremity reveals identical MGL distribution in developing axons (*arrows*). Arrowheads point to the boundary of MGL-sparse axonal segment. *Scale bar* = 20 µm.

Fig. S4 **Primers used to perform quantitative PCR**. (A_1) Isolation of intact RNA is essential for gene expression profiling. Therefore, we ran an aliquot of total RNA (1 µg) isolated from microdissected adult mouse brains (RNeasy Mini kit, Qiagen) on a 1.0% agarose gel with GelGreen™ (Biotium). Sharp 28S and 18S rRNA bands indicate intact total RNA. (A_2) Real-time quantitative PCR (qPCR) reactions were validated by preliminary testing of amplification efficacy and by excluding the possibility of genomic DNA contamination in the presence (+) or absence (-) of reverse transcriptase in parallel and running the samples on 1.5% agarose gel. Data for both CB_1R and GAPDH, a housekeeping gene used as internal standard, are shown. (B) Quantitative PCR reactions have been performed with primer pairs amplifying short fragments for each gene. Primer pairs have been designed to efficiently anneal to nucleotide sequences in mouse.

Fig. S5 **Functional integration of eCB signaling in developing subpallium.** (A) Western analysis of metabolic components of 2-AG signaling networks during successive developmental stages. β-III-tubulin served as protein loading control. (A_1,A_2) Quantitative analysis with each data point representing mean integrated density values (± sem) of DAGLα, MGL and CB_1R, CRIP1a in at least 3 independent experiments. Neonatal (P1) cortical samples were used to normalize expression levels.*$p < 0.05$ (Student's *t*-test).

Fig. S6 **Axonal MGL redistribution during synaptogenesis.** (A) Postsynaptic target selection coincides with MGL redistribution along the axon (*arrowheads*) and the growth cone (1, *arrow*) facing a postsynaptic target (pst). In the meantime, motile axon collaterals lack MGL (2; *open arrowheads*). (B-D_2) Comparative analysis of growth cone morphologies, the presence of postsynaptic targets, and MGL expression during successive stages of synaptogenesis. VAMP2 was used as an early synapse-related marker in differentiating growth cones (Sabo and McAllister, 2003). Note that only stationary growth cones harbor significant quantities of MGL (D-D_2). Solid arrowheads in (B-D_2) mark the MGL gradient, while open arrowheads point to MGL-sparse filopodia. Abbreviations: Supporting information test. *Scale bars* = 15 µm (A), 3 µm (C_2,D_2).

Reference List

Aguado T, Monory K, Palazuelos J, Stella N, Cravatt B, Lutz B, Marsicano G, Kokaia Z, Guzman M, Galve-Roperh I (2005) The endocannabinoid system drives neural progenitor proliferation. FASEB J 19:1704-1706.

Barbin G, Aigrot MS, Charles P, Foucher A, Grumet M, Schachner M, Zalc B, Lubetzki C (2004) Axonal cell-adhesion molecule L1 in CNS myelination. Neuron Glia Biol 1:65-72.

Begbie J, Doherty P, Graham A (2004) Cannabinoid receptor, CB1, expression follows neuronal differentiation in the early chick embryo. J Anat 205:213-218.

Berghuis P, Rajnicek AM, Morozov YM, Ross RA, Mulder J, Urban GM, Monory K, Marsicano G, Matteoli M, Canty A, Irving AJ, Katona I, Yanagawa Y, Rakic P, Lutz B, Mackie K, Harkany T (2007) Hardwiring the brain: endocannabinoids shape neuronal connectivity. Science 316:1212-1216.

Bicknese AR, Sheppard AM, O'Leary DD, Pearlman AL (1994) Thalamocortical axons extend along a chondroitin sulfate proteoglycan-enriched pathway coincident with the neocortical subplate and distinct from the efferent path. J Neurosci 14:3500-3510.

Bisogno T, Howell F, Williams G, Minassi A, Cascio MG, Ligresti A, Matias I, Schiano-Moriello A, Paul P, Williams EJ, Gangadharan U, Hobbs C, Di Marzo V, Doherty P (2003) Cloning of the first sn1-DAG lipases points to the spatial and temporal regulation of endocannabinoid signaling in the brain. J Cell Biol 163:463-468.

Brittis PA, Silver J, Walsh FS, Doherty P (1996) Fibroblast growth factor receptor function is required for the orderly projection of ganglion cell axons in the developing mammalian retina. Mol Cell Neurosci 8:120-128.

De Carlos JA, O'Leary DD (1992) Growth and targeting of subplate axons and establishment of major cortical pathways. J Neurosci 12:1194-1211.

Goncalves MB, Suetterlin P, Yip P, Molina-Holgado F, Walker DJ, Oudin MJ, Zentar MP, Pollard S, Yanez-Munoz RJ, Williams G, Walsh FS, Pangalos MN, Doherty P (2008) A diacylglycerol lipase-CB2 cannabinoid pathway regulates adult subventricular zone neurogenesis in an age-dependent manner. Mol Cell Neurosci in press.

Harkany T, Hartig W, Berghuis P, Dobszay MB, Zilberter Y, Edwards RH, Mackie K, Ernfors P (2003) Complementary distribution of type 1 cannabinoid receptors and vesicular glutamate transporter 3 in basal forebrain suggests input-specific retrograde signalling by cholinergic neurons. Eur J Neurosci 18:1979-1992.

Jacobowitz DM, Abbott LC (1997) Chemoarchitectonic atlas of the developing mouse brain. Boca Raton, FA, USA: CRC Press LLC.

Katona I, Urban GM, Wallace M, Ledent C, Jung KM, Piomelli D, Mackie K, Freund TF (2006) Molecular composition of the endocannabinoid system at glutamatergic synapses. J Neurosci 26:5628-5637.

Keays DA, Tian G, Poirier K, Huang GJ, Siebold C, Cleak J, Oliver PL, Fray M, Harvey RJ, Molnar Z, Pinon MC, Dear N, Valdar W, Brown SD, Davies KE, Rawlins JN, Cowan NJ, Nolan P, Chelly J, Flint J (2007) Mutations in alpha-tubulin cause abnormal neuronal migration in mice and lissencephaly in humans. Cell 128:45-57.

Molnar Z, Metin C, Stoykova A, Tarabykin V, Price DJ, Francis F, Meyer G, Dehay C, Kennedy H (2006) Comparative aspects of cerebral cortical development. Eur J Neurosci 23:921-934.

Morozov YM, Torii M, Rakic P (2009) Origin, early commitment, migratory routes, and destination of cannabinoid type 1 receptor-containing interneurons. Cereb Cortex 19 Suppl 1:i78-i89.

Mulder J, Aguado T, Keimpema E, Barabas K, Ballester Rosado CJ, Nguyen L, Monory K, Marsicano G, Di Marzo V, Hurd YL, Guillemot F, Mackie K, Lutz B, Guzman M, Lu HC, Galve-Roperh I,

Harkany T (2008) Endocannabinoid signaling controls pyramidal cell specification and long-range axon patterning. Proc Natl Acad Sci U S A 105:8760-8765.

Pleasure SJ, Anderson S, Hevner R, Bagri A, Marin O, Lowenstein DH, Rubenstein JL (2000) Cell migration from the ganglionic eminences is required for the development of hippocampal GABAergic interneurons. Neuron 28:727-740.

Riedel A, Hartig W, Seeger G, Gartner U, Brauer K, Arendt T (2002) Principles of rat subcortical forebrain organization: a study using histological techniques and multiple fluorescence labeling. J Chem Neuroanat 23:75-104.

Sabo SL, McAllister AK (2003) Mobility and cycling of synaptic protein-containing vesicles in axonal growth cone filopodia. Nat Neurosci 6:1264-1269.

Straiker A, Hu SS, Long J, Arnold A, Wager-Miller J, Cravatt BF, Mackie K (2009) Monoacyl glycerol lipase (MGL) limits the duration of endocannabinoid-mediated depolarization-induced suppression of excitation (DSE) in autaptic hippocampal neurons. Mol Pharmacol.

Tanaka D, Nakaya Y, Yanagawa Y, Obata K, Murakami F (2003) Multimodal tangential migration of neocortical GABAergic neurons independent of GPI-anchored proteins. Development 130:5803-5813.

Uchigashima M, Narushima M, Fukaya M, Katona I, Kano M, Watanabe M (2007) Subcellular arrangement of molecules for 2-arachidonoyl-glycerol-mediated retrograde signaling and its physiological contribution to synaptic modulation in the striatum. J Neurosci 27:3663-3676.

Walker DJ, Suetterlin P, Reisenberg M, Williams G, Doherty P (2009a) Down-regulation of diacylglycerol lipase-alpha during neural stem cell differentiation: Identification of elements that regulate transcription. J Neurosci Res.

Walker DJ, Suetterlin P, Reisenberg M, Williams G, Doherty P (2009b) Down-regulation of diacylglycerol lipase-alpha during neural stem cell differentiation: Identification of elements that regulate transcription. J Neurosci Res.

Yoshida T, Fukaya M, Uchigashima M, Miura E, Kamiya H, Kano M, Watanabe M (2006) Localization of diacylglycerol lipase-alpha around postsynaptic spine suggests close proximity between production site of an endocannabinoid, 2-arachidonoyl-glycerol, and presynaptic cannabinoid CB1 receptor. J Neurosci 26:4740-4751.

Keimpema. Barabas *et al*. - Supplemental figure 1
(JN-RM-2126-10, revision)

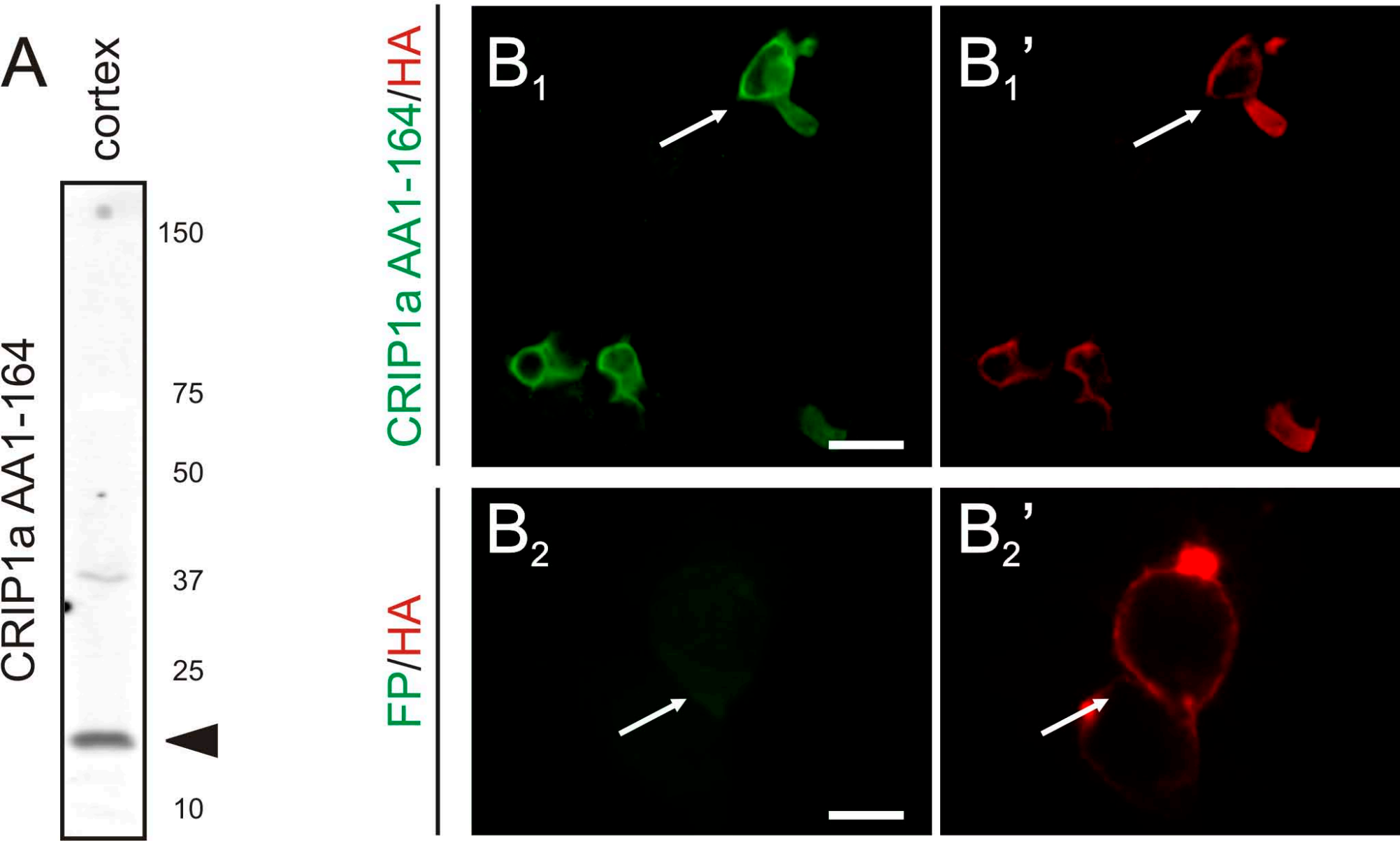

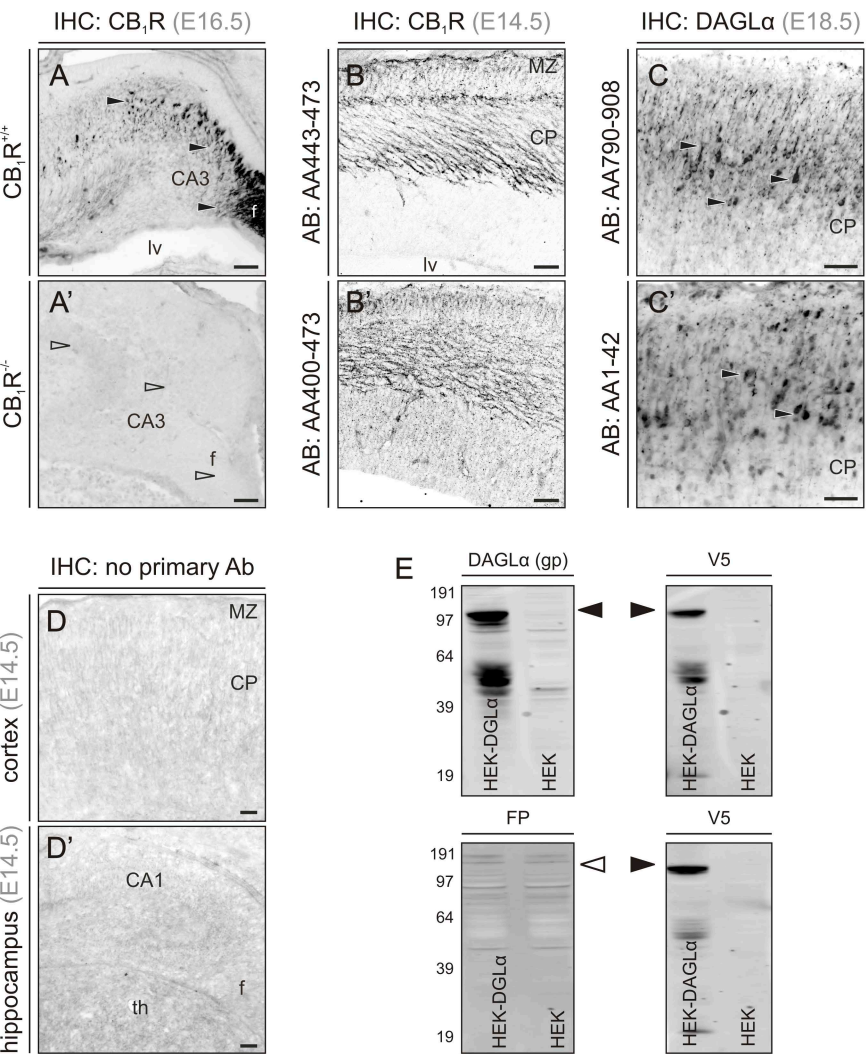
IHC: CB1R (E16.5)
IHC: CB1R (E14.5)
IHC: DAGLα (E18.5)
CB1R+/+
CB1R-/-
A
A'
CA3
f
lv
B
B'
MZ
CP
AB: AA443-473
AB: AA400-473
C
C'
AB: AA790-908
AB: AA1-42
IHC: no primary Ab
D
D'
cortex (E14.5)
hippocampus (E14.5)
CA1
th
E
DAGLα (gp)
V5
FP
191
97
64
39
19
HEK-DGLα
HEK
HEK-DAGLα

Keimpema. Barabas *et al*. - Supplemental figure 3
(JN-RM-2126-10, revision)

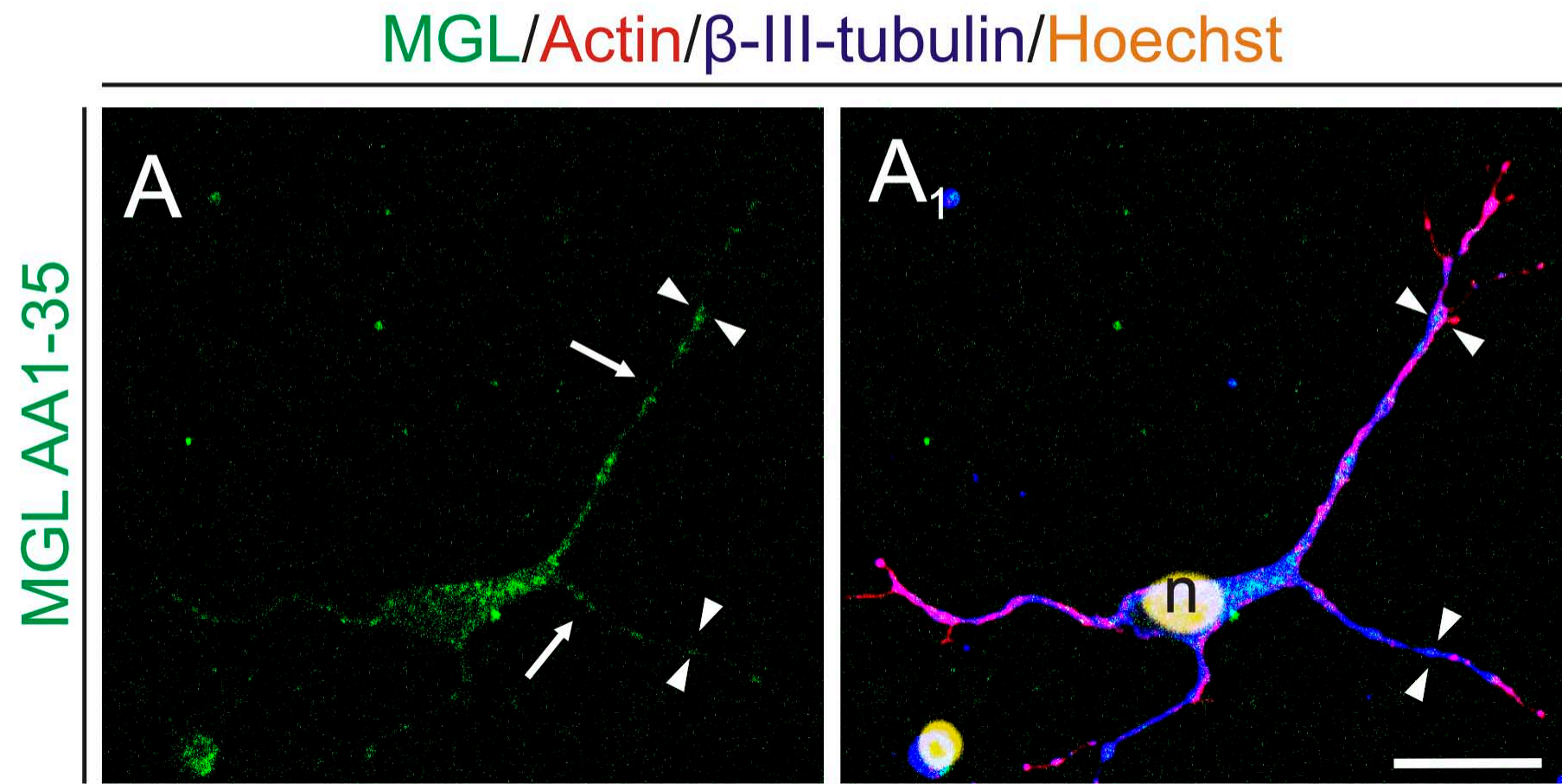

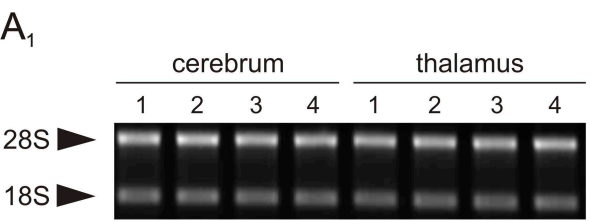

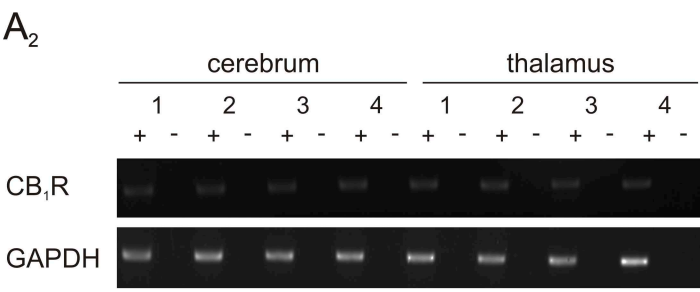

B

GenBank number	Protein	Primer pair[a]	T_A (°C)[b]	Localization
NM_007726	CB_1R	(forward) 5'-TCTTAGACGGCCTTGCAGAT-3' (reverse) 5'-AGGGACTACCCCTGAAGGAA-3'	60	exon 2 exon 2
NM_198114	DAGLα	(forward) 5'-TCATGGAGGGGCTCAATAAG-3' (reverse) 5'-AGCCCTCCAGACTCATCTCA-3'	60	exon 18 exon 20
NM_144915	DAGLβ	(forward) 5'-GTGTGCTGTGGTGGATTGTC-3' (reverse) 5'-TCTCATGCTGACACACACGA-3'	60	exon 1/2 exon 2
NM_011844	MGL	(forward) 5'-CAGAGAGGCCAACCTACTTTTC-3' (reverse) 5'-ATGCGCCCCAAGGTCATATTT-3'	62	exon 2/3 exon 4
NM_008084	GAPDH	(forward) 5'-AACTTTGGCATTGTGGAAGG-3' (reverse) 5'-ACACATTGGGGGTAGGAACA-3'	60/62	exon 5 exon 7

a) 'forward' and 'reverse' indicate primer orientation

b) annealing temperature

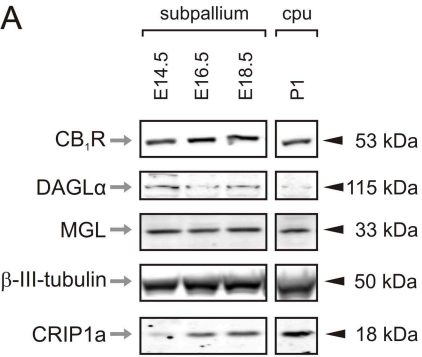
A
subpallium
cpu
E14.5
E16.5
E18.5
P1
CB1R
DAGLα
MGL
β-III-tubulin
CRIP1a
53 kDa
115 kDa
33 kDa
50 kDa
18 kDa

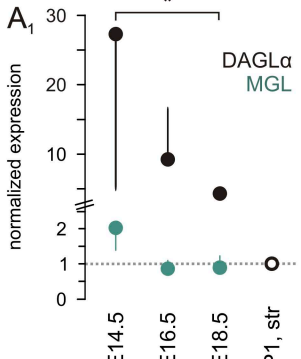
A1
normalized expression
DAGLα
MGL
*
30
20
10
2
1
0
E14.5
E16.5
E18.5
P1, str

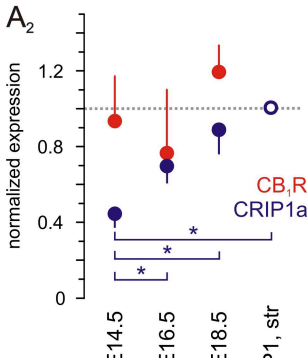
A2
normalized expression
CB1R
CRIP1a
*
*
*
1.2
0.8
0.4
0
E14.5
E16.5
E18.5
P1, str

Keimpema, Barabas *et al*. - Supplemental figure 6 (JN-RM-2126-10, revision)

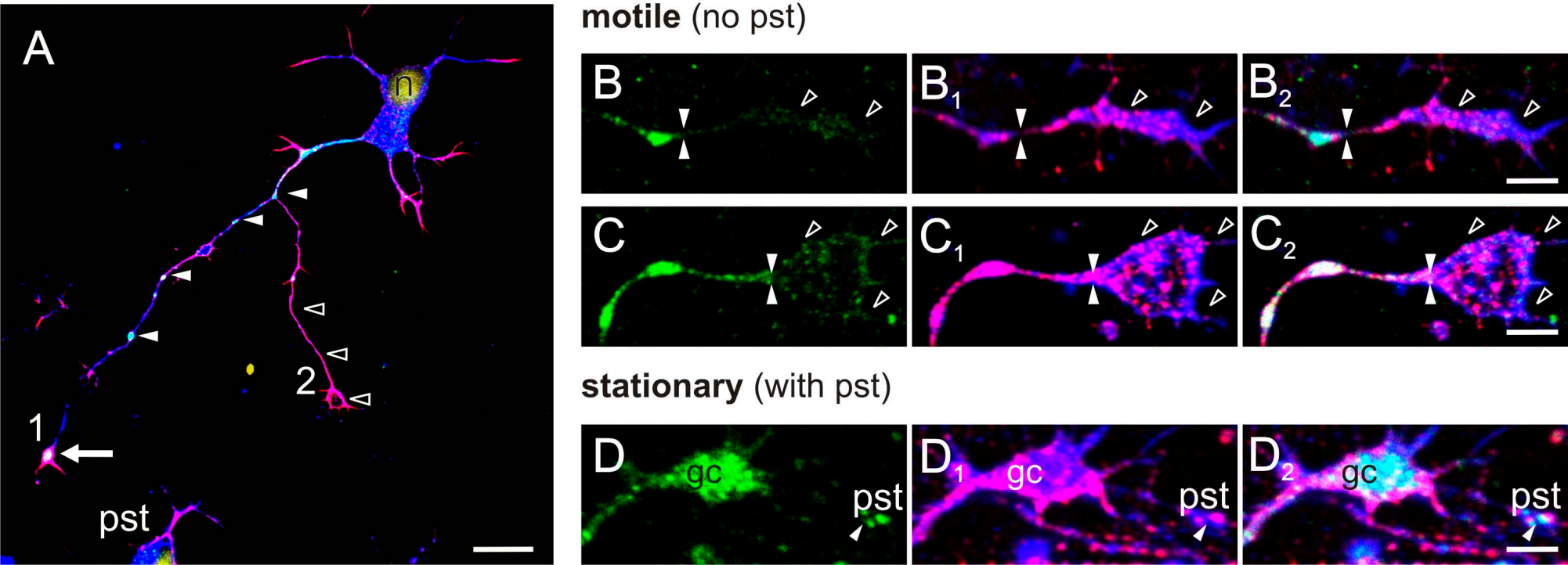

A

Marker	Host	Dilution	Epitope	Reference
CB_1R	goat	1:1,000	AA443-473	Uchigashima *et al* (2007)
CB_1R	guinea pig	1:1,000	AA400-473	Mulder *et al* (2008)
CRIP1a	rabbit	1:2,000	AA1-164	present report
DAGLα	guinea pig	1:1,000	AA790-908	Katona *et al* (2006)
DAGLα	rabbit	1:1,000	AA1016-1042	Katona *et al* (2006)
DAGLα	goat	1:1,000	AA1-42	Yoshida *et al* (2006)
MGL	rabbit	1:1,000	AA1-35	present report
MGL	rabbit	1:1,000	AA171-206	Straiker *et al* (2009)

A_1

Marker	Host	Dilution	Source	Reference
β-III-tubulin	mouse	1:2,000	Promega	Berghuis *et al* (2007)
Brn-1	goat	1:1,000	Santa Cruz	Keays *et al* (2007)
L1-NCAM	rat	1:1,000	Millipore	Barbin *et al* (2004)
Phalloidin (F-actin)		1:500	Invitrogen	Berghuis *et al* (2007)
VAMP2	mouse	1:1,000	Synaptic S.	Sabo *et al* (2003)